Journal of Alloys and Compounds 516 (2012) 161–166

Contents lists available at SciVerse ScienceDirect

Journal of Alloys and Compounds

journal homepage: www.elsevier.com/locate/jallcom

Fabrication of CuW pseudo alloy by W–CuO nanopowders

Shuhua Liang*, Xianhui Wang, Lingling Wang, Weichan Cao, Zhikang Fang

School of Materials Science and Engineering, Xi'an University of Technology, 5 South Jinhua Road, Xi'an, Shaanxi 710048, PR China

ARTICLE INFO

Article history:
Received 10 November 2010
Received in revised form 2 December 2011
Accepted 6 December 2011
Available online 16 December 2011

Keywords:
CuW pseudo alloy
Skeleton
Infiltration
Sintering
Properties
Arcing

ABSTRACT

CuW pseudo alloy was fabricated with W–CuO nanopowders by sintering and infiltration. The microstructure and phase constituents of the CuW pseudo alloy prepared were characterized by a scanning electron microscope, X-ray diffractometer, and the arc erosion behavior was also evaluated by arcing test. The CuO powders, instead of the induced copper powders, were introduced into W nanopowders. CuW pseudo alloy with uniform structures of Cu and W phases was obtained when 11 wt.% CuO powders were introduced into W nanopowders. In comparison to the conventional CuW pseudo alloy, the sizes of W skeleton and the infiltrated Cu phase were reduced remarkably and both the hardness and electrical conductivity were increased. The arc erosion resistance was increased due to the split characteristic of the cathode spot for the CuW pseudo alloy prepared by W–CuO nanopowders. The appropriate addition of induced copper can improve the distribution of Cu and W phases, and promote the subsequent infiltration of the molten Cu due to pre-wetting the surface of W skeleton.

1. Introduction

Due to the good combination of the intrinsic properties of both W and Cu constituents, CuW pseudo alloys are widely used as high voltage electrical contacts, resistance welding electrode, electronic packaging materials and nozzle liner in rockets and missiles. Among these applications, the most successful example is that they are used as electrical contact materials in the high voltage breakers [1–4]. As one of the key components in the high voltage breakers, the electrical contact performs the switch on–off operation. During service, the electrical contact not only transports huge current once the switch on is established, but also suffers from high-temperature arc erosion as well. With increase of the power grid load and interruption capacity, it is imperative for the stringent arc erosion resistance of the electrical contact materials [1,5].

For CuW pseudo alloy, Cu and W phase play different roles during arcing. Cu phase can disperse arc motion and release the heat by self-vaporization, resulting in less burning loss; while W skeleton suffers the impact from arc, and provides capillary force to prevent the splash of the molten Cu, thus reducing the arc erosion. Therefore, it is required that W skeleton should have a sufficient strength and capillary force at elevated temperatures, and Cu phase should have a fine well-dispersed distribution in W matrix. Subsequently, mechanical properties as well as electrical properties of the contact materials largely depend on both the continuity of skeleton and the distribution of copper [1,5–7]. Generally, some tiny addition of alloying elements, such as Ni,Co,Cr, into W matrix can improve the strength of W skeleton since they can form a special thin film on the surface of W grains and promote the diffusion of W and activated sintering [8–12]. Nevertheless, it is noted that the addition of Ni may form Ni_4W and reduce the electrical and thermal conductivity [11,13]. In addition, some new preparation methods have been reported to fabricate CuW pseudo alloy, such as microwave sintering, injection molding and field-assisted sintering [3,14–17].

Recently, more attentions are paid on the production of CuW pseudo alloy with fine microstructure through sintering Cu–W nanopowders prepared by chemical methods [2,18–23]. One way to prepare CuW nanopowders is through calcinations and H_2 reduction utilizing $(NH_4)_6(H_2W_{12}O_{40})\cdot 4H_2O$, $Na_2WO_4\cdot 2H_2O$, $Cu_2WO_4(OH)_2$, $CuWO_4\cdot 2H_2O$ and $[Cu(NO_3)_2]\cdot 3H_2O$ as raw materials; and another way to prepare Cu–W nanopowders is through milling WO_3 and CuO powders followed by H_2 reduction. CuW pseudo alloys were fabricated by pressing and subsequent sintering the compact of Cu–W nanopowders. Due to no addition of any activation agent in the manufacturing process, the CuW pseudo alloy has higher purity, larger hardness and better electrical conductivity along with more homogeneous distribution of superfine Cu phase among W particles, which can be used as high power electrical packaging and heat sink materials. Nevertheless, it is difficult to get the desired bi-continuous microstructures as W particles are entirely separated by Cu nanoparticles in the CuW pseudo alloys.

In the present investigation, to obtain CuW contact materials with a bi-continuous microstructure of Cu and W phase, a W skeleton with a bicontinuous structure of W particles and pores were fabricated beforehand by introducing small amounts of induced Cu powders, followed by infiltrating Cu into the W skeleton. The

* Corresponding author. Tel.: +86 29 82312181; fax: +86 29 82312181.
E-mail address: liangsh@xaut.edu.en (S. Liang).

0925-8388/$ – see front matter © 2011 Elsevier B.V. All rights reserved.
doi:10.1016/j.jallcom.2011.12.018

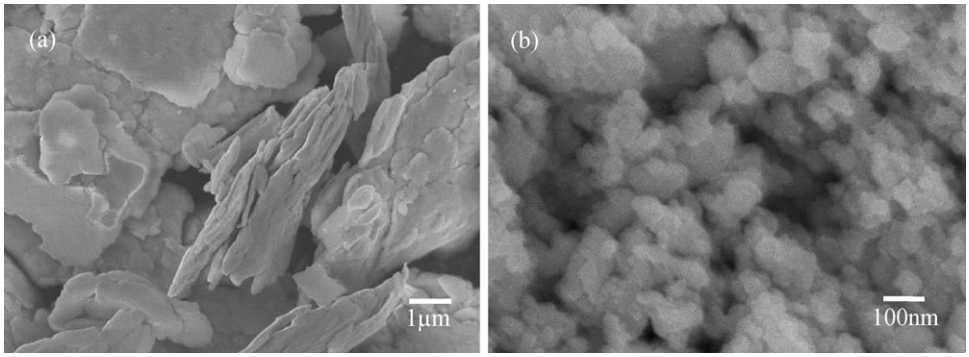

Fig. 1. The morphologies of pure Cu and CuO milled powders: (a) Cu and (b) CuO.

results demonstrated a promising way to make a CuW pseudo alloy with a high purity, high hardness, good electrical conductivity and a desired bicontinuous microstructure of fine W and Cu phase.

2. Experimental procedures

In the present study, the mixture of W and CuO nanopowders was first milled, and then reduced into W and Cu powders. The reduced W and Cu powders were pressed into a compact, followed by sintering to prepare W skeleton with preformed pores. Finally, CuW70 pseudo alloy was fabricated by infiltrating molten Cu into the W skeleton.

CuO powders (99.9%, 20–40 nm, Shanghai Jinzheng metal powders Co., LTD., China) and W powders (99.9%, 80–100 nm, Xiamen golden egret special alloy Co., LTD., China) were used as original materials. 3–15 wt.% CuO powders used as induced copper powders were first milled with W powders for 4 h. The milled W–CuO mixture was reduced under dry H_2 atmosphere at 600–800 °C for 2 h. The reduced powders were subsequently pressed uniaxially. In this experiment, a rigid washer was used to control the height of the compacts, i.e. when the compacts were pressed to the designed height, more pressure can only be applied on the rigid washer. The pressure was in the range of 100–150 MPa. The mass of W–Cu powder mixtures were 72.06 g, 76.30 g and 79.13 g, respectively, which were corresponded to the original content of induced CuO powders (3%, 11%, 15%). The size of W skeleton specimens was Φ 30 mm × 10 mm. These W skeleton specimens were sintered at 900 °C for 1 h (heating rate 15 °C/min) in hydrogen atmosphere, and infiltrated with Cu at 1250 °C for 1 h to obtain CuW70 pseudo alloy. In order to compare the morphologies of milled CuO and Cu, pure Cu powders were also milled using the same milling parameters.

The phase constituents of hydrogen-reduced W–Cu mixture were determined by a XRD-7000 X-ray diffractometer with Cu Kα radiation (λ = 0.15406 nm). The microstructures of reduced W–Cu mixture and CuW pseudo alloy were characterized by a JSM-6700F scanning electron microscope (SEM). The electrical conductivity was tested by a 7501 eddy-current conductivity instrument, and the hardness test was performed on a HB-3000 Brinell hardness tester under the load of 750 kg holding for 30 s. The density was measured utilizing Archimedean method. The arc behaviors between anode and cathode were observed and recorded by a digital high-speed video camera, Phantom V9, in which the set-up resolution and sampling rate were 192 × 64 dpi and 24,000 f/s, respectively. The concentration of Cu in CuW pseudo alloy was analyzed by a chemical method, i.e., CuW sample was first dissolved in the solution of sulfuric acid and ammonium sulfate, followed by the addition of potassium iodide solution, and then Cu^{2+} can be reduced into Cu along with the precipitation of equivalent iodine. In the process, starch-liquefying was utilized as the indicator, and the copper content was determined by the titration volume of standard solution of sodium thiosulfate.

3. Results and discussion

3.1. Preparation of W–Cu powders

3.1.1. Preparation of W–CuO mixture

In order to get an interconnected W skeleton with well-distributed pores after sintering W nanopowders, small amounts of Cu nanopowders are introduced into W nanopowders before sintering. Due to large specific surfaces and high surface energy of nanopowders, it is easier to cause the aggregation of powders. High energy milling is a good approach to achieve a uniform distribution of W and Cu.

The morphologies of pure Cu and CuO milled powders are shown in Fig. 1(a) and (b), respectively. It can be seen from Fig. 1(a) that pure Cu powders exist in the form of a laminar shape after milling due to its soft and ductile characteristics. If pure Cu powders and nanometers W powders are mixed by high energy ball milling, the mixture of Cu and W powders maybe present in the form of the laminar or flake shape. This specific morphology might be inherited in the subsequent sintering and infiltration, resulting in the formation of copper rich phase.

However, this phenomenon is not observed in CuO milled powders. As seen from Fig. 1(b), CuO powders present in the form of spherical nanometer particles after milling. Moreover, spherical particles have better fluidity. Hence, CuO powders, instead of Cu powders, were used in this investigation.

Fig. 2 is SEM images of W–CuO mixture and the mapping results of W and Cu. As seen from Fig. 2, no aggregation can be observed, along with the disappearance of irregular particles, CuO powders are dispersed uniformly among W powders. Due to the large brittleness of W and CuO powders, the adhesive forces of their aggregate are not as strong as that of ductile metallic powders. Under repeated impact and extrusion, it is easy for those aggregate to be broken. At the subsequent stage, it is subjected to a series of process, such as deformation, cold welding and rupture, which are quite similar to metallic powders during the mechanical alloying process. After milling, a large amount of fresh surface and well-bonded surface are formed, and CuO particles are embedded into W matrix as well. Thus, W nanoparticles could be separated effectively to obtain a uniform mixture of W and CuO.

3.1.2. Processing of W–Cu nanopowders

CuO powders should be reduced by H_2 before sintering W skeleton in this investigation. The reduction temperature of CuO was first determined by thermodynamics. The reaction equations are as follows.

$$2H_{2(g)} + O_{2(g)} = 2H_2O_{(g)} \quad \Delta G^0 = A + BT = -499,200 + 114.2T \tag{1}$$

$$2Cu_{(s)} + O_{2(g)} = 2CuO_{(s)} \quad \Delta G^0 = A + BT = -311,700 + 180.3T \tag{2}$$

According to Eqs. (1) and (2), the following equation can be obtained.

$$CuO_{(s)} + H_{2(g)} = Cu_{(s)} + H_2O_{(g)} \quad \Delta G^0 = -93,750 - 33.05T \tag{3}$$

A reduction reaction can occur when $\Delta G \leq 0$. i.e.

$$\Delta G = \Delta G^0 + RT \ln Q = -93,750 - 33.05T + RT \ln Q \leq 0 \tag{4}$$

where Q is a partial pressure entropy, $Q = (P_{H_2O} \cdot a_{Cu})/P_{H_2} \cdot a_{CuO}$, a_{CuO} and a_{Cu} are activity coefficient of CuO and Cu, respectively.

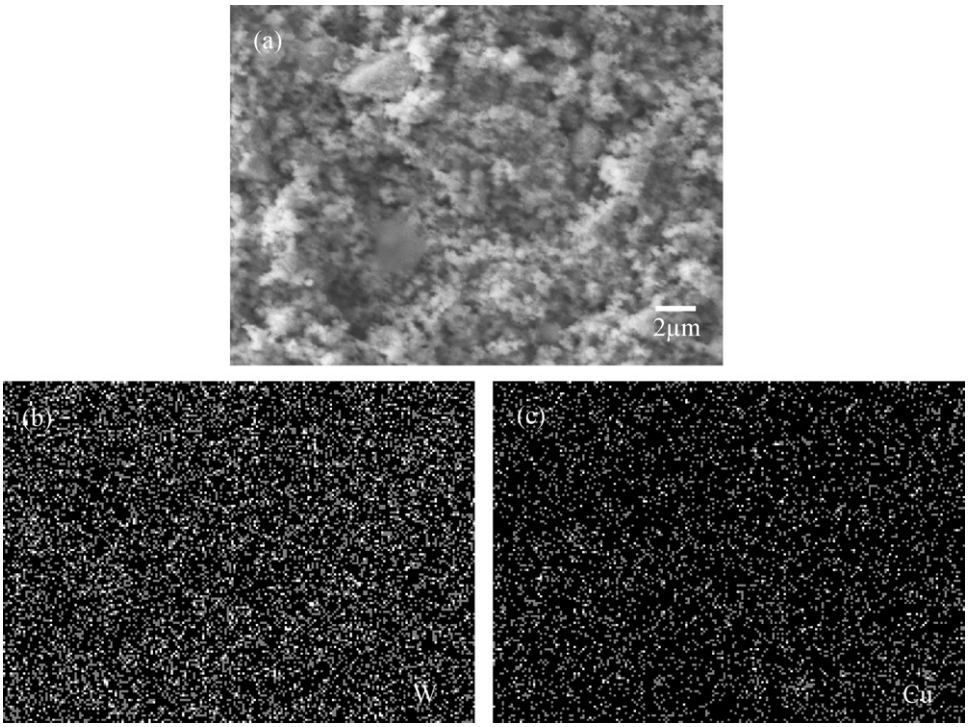

Fig. 2. SEM micrograph and the mapping result of W + CuO powders milled for 4 h.

As both Cu and CuO are pure condensed matter, $a_{CuO} = a_{Cu} = 1$, so $Q = P_{H_2O}/P_{H_2}$.

From Eq. (4), ΔG mainly depends on P_{H_2O}. As H_2 pressure is about 1.3 atm in the actual reduction process, and the partial pressure of water vapor is very small, $RT \ln Q$ has a less effect on ΔG. In addition, the first two items in Eq. (4) are always less than zero. Therefore, based on thermodynamics theory, CuO can be reduced by H_2 at any temperature. Whereas, according to kinetics theory, some thermal energy is needed for the occurrence of the reduction reaction as it is an endothermic reaction. In this work, CuO reduction reaction was studied at 600 °C, 700 °C and 800 °C.

Fig. 3 is the XRD patterns of W–CuO mixture reduced at different temperatures, and the inset is the morphology of reduced powders. As seen from Fig. 3, Cu_2O, WO_2 and WO_3 peaks present after reducing at 600 °C. Cu_2O should be the primary reduced product of CuO, while WO_2 and WO_3 may derive from raw materials and milling process due to the large activity of W nanopowders. It suggests that W–CuO mixture cannot be totally reduced at 600 °C. At 700 °C, other oxides peaks disappear and only W peaks present without the presence of Cu and CuO peaks. However, the present authors still believe that only partial CuO powders have been reduced since their contents are too low beyond the detection range of XRD diffractometer. Therefore, only W peaks are detected, and no Cu peaks present at 700 °C.

When the reduction temperature reaches up to 800 °C, CuO and Cu_2O peaks disappear, Cu peaks appear and the intensity of W peaks becomes stronger, indicating that W–CuO mixture can be entirely reduced at 800 °C. After reduction, the particle sizes are around 100 nm, and no W aggregation and growth are presented due to the well-dispersed Cu. In this experiment, the size of Cu particles reduced from the milled CuO powders was in the magnitude of nanometer, and its content was far below the content of tungsten matrix. Additionally, the samples used for XRD analysis were powders, along with diffraction limited accuracy. Therefore, only main strong peaks of copper are presented without other peaks in the XRD pattern.

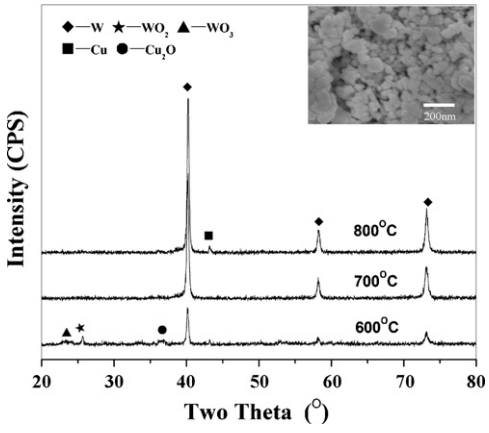

Fig. 3. XRD patterns of W + CuO powders at different temperatures, and the inset is the SEM image of reduced W + CuO powders.

3.2. Preparation of CuW pseudo alloys

CuW pseudo alloys were fabricated by compacting the reduced CuO–W powders, sintering and infiltrating the molten Cu. The final Cu content, hardness, electrical conductivity and density of CuW pseudo alloys prepared are given in Table 1. It is learnt from Table 1

Table 1
Properties of CuW pseudo alloys with different CuO contents.

CuW	Conventional CuW pseudo alloy	3% CuO	11% CuO	15% CuO
Hardness (HB)	178	201	194	185
Electrical conductivity (ms/m)	23	20	24	26
Relative density (%)	98.9	94.5	98.7	98.8
Content of copper (wt.%)	29.5	26.9	29.3	32.7

that the content of primary CuO has a significant effect on the properties of CuW pseudo alloy. With an increase of the content of primary CuO, the final Cu content obtained in the CuW pseudo alloy increases, and the electrical conductivity and relative density increase as well. However, the hardness decreases. Although there are the most important effect of the primary CuO content on the final properties such as hardness, electrical conductivity and relative density, the microstructural evolutions can affect the changes in properties, either.

3.2.1. Effect of the induced Cu content on sintering

In the present study, the CuO powders introduced in W nanopowders are used as the substitute of the induced copper powders. They not only change the distribution and amount of the preformed pores in W skeleton, but also promote the molten Cu infiltration into W skeleton during subsequent fabrication process.

Fig. 4(a)–(c) is the morphologies of CuW pseudo alloys prepared by adding 3 wt.%, 11 wt.% and 15 wt.% CuO, reducing at 800 °C under H_2, sintering and infiltration. The inset in Fig. 4(b) is the morphology of W skeleton before infiltration. Fig. 5 is the X-ray diffraction pattern of the CuW pseudo alloy prepared by the addition of 11 wt.% CuO. As seen from Fig. 5, the final CuW pseudo alloy is consisted of copper and tungsten phase. From Fig. 4, the continuous light gray regions represent W phase while black regions represent Cu phase. It can be seen from Fig. 4 that the CuW pseudo alloy prepared has a bicontinuous structure. This morphology of CuW pseudo alloy is beneficial as the high voltage electrical contact as discussed in the introduction. The role of induced copper powders can be further explained as follows.

Without the addition of the induced Cu powders, the contacts among W particles before and after sintering are shown in Fig. 6(a) and (b), respectively. With the appropriate addition of induced Cu powders, the contacts among W particles before and after sintering are shown in Fig. 6(c) and (d), respectively. Fig. 6(e) and (f) represents the contacts among W particles before and after sintering when excessive induced Cu powders are added. When no induced coppers are introduced into the W powders compact during sintering, the point contact progressively evolves into surface contact under the action of surface atom diffusion and surface tension, and a dense sinter with the closed pores are finally formed by a number of W particles. The closed pores will prohibit the infiltration of molten Cu. Especially for the sintering of W nanopowders, it becomes more remarkable due to the higher surface energy of nanopowders, as shown in Fig. 6(a) and (b).

An appropriate addition of the induced Cu powders can partially separate the W nanopowders effectively, thus avoiding the formation of rich W phase and closed pores. Nanopowders are at least connected together in one direction to form W continuous skeleton, as seen in Fig. 6(c) and (d). At elevated infiltration temperatures, the induced Cu powders in the porous W skeleton are firstly melted and wet the W skeleton, which can favor for the infiltration of the molten Cu and uniform distribution of W and Cu phase, as shown in Fig. 4(b). Whereas, as seen in Fig. 6(e) and (f), an excessive Cu addition causes the full separation of W particles, resulting in the formation of a disconnected W skeleton during sintering. During subsequent infiltration, the disconnected W skeleton will cause partial collapse, resulting in a serious aggregation of W or Cu, and formation of the worse microstructure, as shown in Fig. 4(d).

3.2.2. Effect of the induced Cu content on the properties of CuW pseudo-alloy

From Table 1, it is learnt that the content of CuO has a significant effect on the properties of CuW pseudo alloy. When 3 wt.% CuO is added, the electrical conductivity and relative density are low, the hardness is high, and the final content of Cu is only 26.9% (given in Table 1), which is lower than the designed 30% Cu in CuW pseudo alloy. This can be ascribed to the rapid sintering of nanometer tungsten powders with few Cu barriers, and the formation of dense tungsten skeleton and some blind holes, thus prohibiting Cu sufficient infiltration. So both the electrical conductivity and relative density decrease, as shown in Fig. 4(a).

At an addition of the 11 wt.% CuO, the electrical conductivity and relative density are enhanced. The final content of Cu (29.6 wt.%) is in good agreement with the designed content of 30 wt.% Cu in CuW pseudo alloy. Compared with the CuW pseudo alloy prepared by

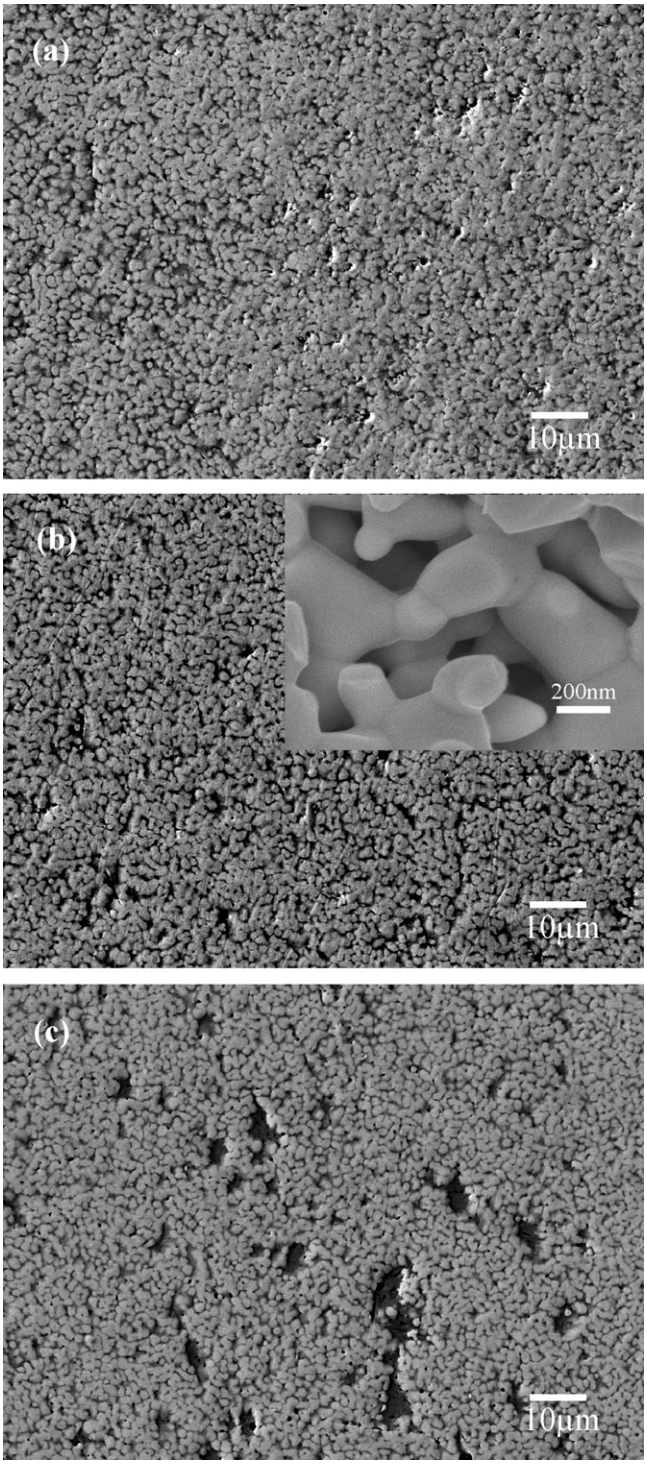

Fig. 4. SEM images of CuW pseudo alloys prepared with different CuO contents: (a) 3 wt.% CuO; (b) 11 wt.% CuO; (c) 15 wt.% CuO.

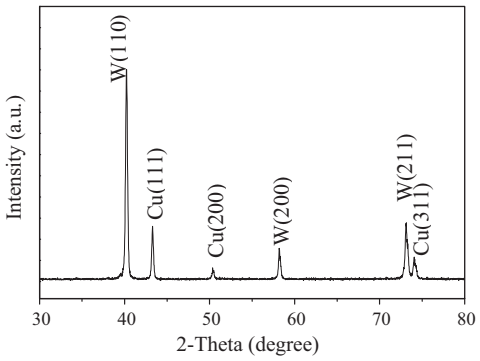

Fig. 5. X-ray diffraction pattern of the final CuW pseudo alloys.

the addition of 3 wt.% CuO, the hardness decreases. This is mainly due to lower content of tungsten.

As shown in Fig. 4(b), no aggregation of tungsten phase can be observed, and the continuous and interconnected W skeleton is formed after sintering. The desired morphology is beneficial for the sufficient infiltration of molten Cu, the improvement of the distribution of W and Cu, and the reduction of micro-structural defects. At 15 wt.% CuO, the final Cu content obtained in CuW pseudo alloy exceeds the designed content of 30% Cu. Obviously, the increase in Cu content decreases the hardness. Nevertheless, the deterioration of microstructure during sintering caused by excess Cu particles around W powders could contribute to the decrease in hardness. In fact, poor sintering of the tungsten powders due to too many Cu barriers around, results in a loose W skeleton and larger size Cu phase and, thus, lower hardness and the highest electrical conductivity.

As discussed above, the content of the induced Cu powders can obviously affect the amount and distribution of pores, structure and size of sintered W skeleton. And the subsequent Cu infiltration will be further affected. Hence, an appropriate content of induced Cu powders is important for the fabrication of CuW pseudo alloy with high quality.

Based on the China national standard No. GB8320-2003, when CuW70 pseudo alloy is prepared by sintering and infiltration, the final content of Cu in CuW pseudo alloy should be 30 ± 2 wt.%. Therefore, the addition of 11 wt.% CuO is the optimum content for the designed content of Cu in the prepared CuW pseudo alloy.

Fig. 7 is the morphology of CuW pseudo alloy prepared by conventional method. Its properties are also given in Table 1. Compared

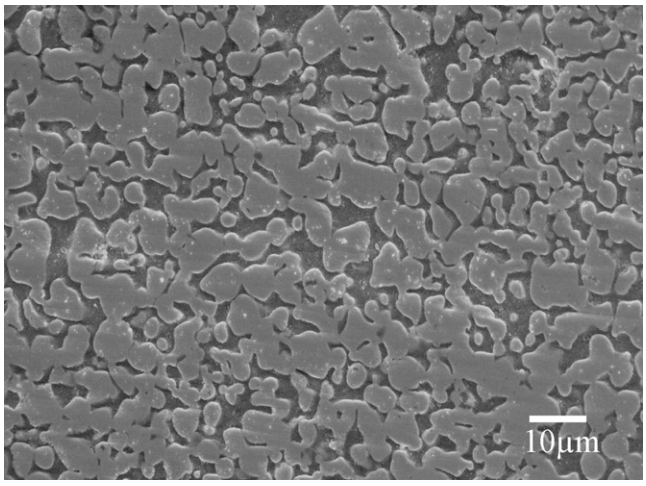

Fig. 7. SEM image of conventional CuW70 pseudo alloy.

with the CuW pseudo alloy prepared with 11 wt.% CuO (under the same final Cu content), both the hardness and electrical conductivity of CuW pseudo alloy prepared with W–CuO nanopowders are larger than those of conventional CuW pseudo alloy, while the relative density has only a slight decrease. This change can be explained as follows. For conventional CuW pseudo alloy, the ligament width of W skeleton and the size of Cu phase are on the magnitude of micron. Nevertheless, for the CuW pseudo alloy prepared with W–CuO nanopowders, the sizes of W skeleton and Cu phase decrease remarkably. The ligament width of W skeleton and the size of Cu phase are sub-micron scales, as shown in Fig. 4(b). Hence, the hardness of the CuW pseudo alloy prepared with W–CuO nanopowders is larger than that of the conventional CuW pseudo alloy. In addition, the better electrical conductivity can be ascribed to no addition of any activating agent into W skeleton during sintering. A slight decrease of the density for CuW pseudo alloy prepared with W–CuO nanopowders may be caused by few blind pores, which have a less effect on the electrical conductivity and hardness.

For electrical contact materials, arc erosion resistance is one of the most important performances to evaluate whether they are suited for the actual applications. Previous studies [5] show that the arc concentration erosion is the main reason to cause the failure of contact materials. In the present investigation, the

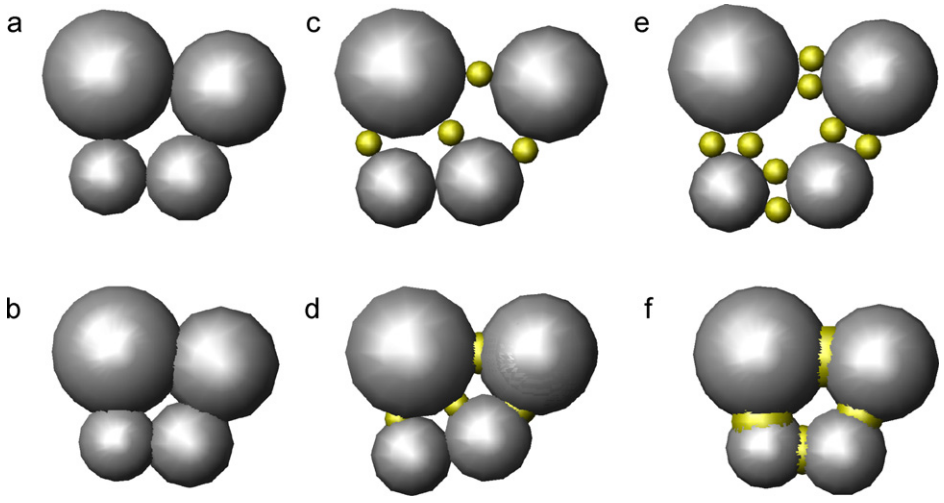

Fig. 6. Schematic of the W skeleton sintering process, (a) and (b) without addition of induced copper before and after sintering, (c) and (d) an appropriate addition of induced copper before and after sintering, (e) and (f) an excessive addition of induced copper before and after sintering.

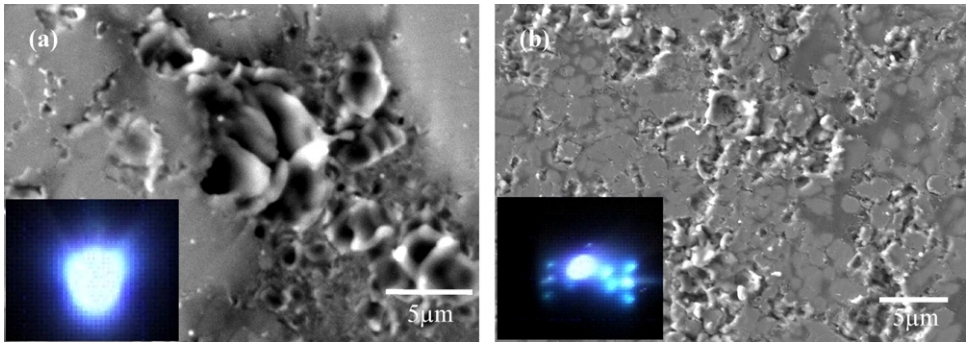

Fig. 8. The surface erosion morphologies of conventional CuW pseudo alloy and sub-micron sized CuW pseudo alloy, and the insets are the morphologies of typical cathode spots (a) conventional CuW pseudo alloy [21] and (b) sub-micron sized CuW pseudo alloy.

arc erosion behavior was studied utilizing a Phantom V9 digital high-speed video camera. Fig. 8(a) and (b) is the surface erosion morphologies of conventional CuW pseudo alloy and sub-micron sized CuW pseudo alloy after arcing test, respectively. The insets are the morphologies of typical cathode spots recorded by the digital high-speed video camera.

For conventional CuW pseudo alloy, it can be seen from Fig. 8(a) that the erosions mainly occur on Cu rich region, and the erosion pits are deep, along with Cu splash on the edge of those pits. It suggests that arc erosions are usually concentrated on Cu rich regions, and the accumulated heat also cause serious partial Cu melt and splash. Nevertheless, for sub-micron sized CuW pseudo alloy, the well-dispersed arc erosion pits are mainly focused on Cu phase and the interface of Cu and W. This change of the morphology of erosion pits derives from the different motion behaviors of cathode spots.

As seen from the insets in Fig. 8, only a single cathode spot presents in the conventional CuW pseudo alloy, and, apparently, its erosion area is concentrated and the depth is larger than that in the sub-micron sized CuW pseudo alloy. However, the cathode spot of the sub-micron sized CuW pseudo alloy are splitted into many tiny spots, thus resulting in the well-dispersed erosion pits. This derives from fine well-dispersed Cu phase and the interface. The cathode spots can simultaneously generate on the adjacent multipoint, thus reducing the arcing current and causing the split of the cathode spots. Subsequently, the sub-micron sized CuW pseudo alloy has a well-dispersed erosion pits and less concentration erosion.

4. Conclusions

(1) A well-distributed mixture of W and Cu nanopowders can be obtained through reduction reaction of the nanosized W and CuO powders by hydrogen at 800 °C.
(2) The appropriate addition of the induced copper can improve the distribution of pores during pressing, prohibit the severe aggregation of tungsten particles during sintering, and promote the subsequent molten Cu infiltration.
(3) In the present study, the CuO powders introduced into W nanopowders are used as the substitute of induced copper powders. Within the range of the experiment, the optimum CuO content is 11 wt.%, at which the final copper content of CuW70 pseudo alloy meets for designed one, and the hardness and electrical conductivity of the prepared CuW pseudo alloy are enhanced.
(4) The ligament width and the size of Cu phase of CuW pseudo alloy prepared with W–CuO nanopowders are the magnitude of sub-micron. The sub-micron sized CuW pseudo alloy presents the split characteristic of cathode spots and less arc concentration erosion.

Acknowledgements

The authors would like to acknowledge the National Natural Science Foundation of China (No. 50871085) and the Key Program of National Natural Science Foundation of China (No. 50834003). This research is also partially supported by Shaanxi Natural Science Foundation (No. 2010JZ007) and Shaanxi Provincial Project of Special Foundation of Key Disciplines.

References

[1] Z.K. Fan, S.H. Liang, P. Xiao, High Voltage Electrical Contact Materials, China Machine Press, 2004, pp. 1–4.
[2] M. Hashempour, H. Razavizadeh, H.R. Rezaie, M. Hashempour, M. Ardestani, Mater. Chem. Phys. 123 (2010) 83–90.
[3] Y. Guo, J. Yi, S. Luo, C. Zhou, L. Chen, Y. Peng, J. Alloys Compd. 492 (2010) L75–L78.
[4] Z. Wang, X. Li, J. Zhu, F. Mo, C. Zhao, L. Wang, Mater. Sci. Eng. A 527 (2010) 6098–6101.
[5] Y. Su, W. Chen, F. Wang, B. Ding, Mater. Lett. 59 (2005) 1046–1049.
[6] J.L. Johnson, S.J. Park, Y.-S. Kwon, R.M. German, Metall. Mater. Trans. A 41 (2010) 1564–1572.
[7] M. Amirjan, N. Parvin, K. Zangeneh-Madar, Mater. Sci. Eng. A 527 (2010) 6922–6929.
[8] N.M. Hwang, Y.J. Park, D.Y. Kim, D.Y. Yoon, Scripta Mater. 42 (2000) 421–425.
[9] A. Ghaderi Hamidi, H. Arabi, S. Rastegari, Int. J. Refract. Met. Hard Mater. 29 (2011) 538–541.
[10] X.H. Yang, Y. Gao, P. Xiao, S.H. Liang, Mater. Sci. Eng. A 528 (2011) 3883–3889.
[11] K.G. Vivek, D.H. Yoon, H.M. Meyer, J. Luo, Acta Mater. 55 (2007) 3131–3142.
[12] A. Genç, S. Coşkun, M.L. Öveçoğlu, J. Alloys Compd. 497 (2010) 80–89.
[13] S. Inomata, M. Kajihara, J. Alloys Compd. 509 (2011) 4958–4966.
[14] D.D. Gu, Y.F. Shen, J. Alloys Compd. 473 (2009) 107–110.
[15] J. Cheng, L. Wan, Y. Cai, J. Zhu, P. Song, J. Dong, J. Mater. Process. Technol. 210 (2010) 137–142.
[16] S. Luo, J. Yi, Y. Guo, Y. Peng, L. Li, J. Ran, J. Alloys Compd. 473 (2009) L5–L9.
[17] A. Rape, S. Chanthapan, J. Singh, A. Kulkarni, J. Mater. Sci. 46 (2011) 94–100.
[18] .D.G. Kim, S.T. Oh, J. Alloys Compd. 354 (2003) 239–242.
[19] H. Abbaszadeh, A. Masoudi, H. Safabinesh, M. Takestani, Int. J. Refract. Met. Hard Mater. 30 (2012) 145–151.
[20] S.H. Hong, B.K. Kim, Mater. Lett. 57 (2003) 2761–2767.
[21] M. Hashempour, H. Razavizadeh, H. Rezaie, Wear 269 (2010) 405–415.
[22] M. Ardestani, H. Arabi, H.R. Rezaie, H. Razavizadeh, Int. J. Refract. Met. Hard Mater. 27 (2009) 796–800.
[23] D.-G. Kim, G.-S. Kim, M.-J. Suk, S.-T. Oh, Y.D. Kim, Scripta Mater. 51 (2004) 677–681.